Nitrate modulates stem cell dynamics
by regulating *WUSCHEL* expression through cytokinins

Authors: Benoit Landrein[1], Pau Formosa-Jordan[1], Alice Malivert[1], Christoph Schuster[1], Charles W. Melnyk[1], Weibing Yang[1], Colin Turnbull[2], Elliot M. Meyerowitz[1,3], James C.W. Locke[1], Henrik Jönsson[1,4,5]

[1] Sainsbury Laboratory, University of Cambridge, Bateman Street, Cambridge CB2 1LR, UK.
[2] Department of Life Sciences, Imperial College London, London SW7 2AZ, UK.
[3] Howard Hughes Medical Institute and Division of Biology and Biological Engineering, California Institute of Technology, Pasadena, CA 91125, USA.
[4] Computational Biology and Biological Physics Group, Department of Astronomy and Theoretical Physics, Lund University, S-221 00 Lund, Sweden.
[5] Department of Applied Mathematics and Theoretical Physics, University of Cambridge, Cambridge CB3 0DZ, UK.

Correspondence: Henrik Jönsson, James C.W. Locke, Elliot M. Meyerowitz,
henrik.jonsson@slcu.cam.ac.uk (H.J.), james.locke@slcu.cam.ac.uk (J.C.W.L.), meyerow@caltech.edu (E.M.M.)

The shoot apical meristem (SAM) is responsible for the generation of all of the aerial parts of plants[1]. Given its critical role, dynamical changes in SAM activity should play a central role in the adaptation of plant architecture to the environment[2]. Using quantitative microscopy, grafting experiments and genetic perturbations, we connect the plant environment to the SAM, by describing the molecular mechanism by which cytokinins signal the level of nutrient availability to the SAM. We show that a systemic signal of cytokinin precursors[3] mediates the adaptation of SAM size and organogenesis rate to the availability of mineral nutrients by modulating the expression of *WUSCHEL*, a key regulator of stem cell homeostasis[4]. In time-lapse experiments, we further show that this mechanism allows meristems to adapt to rapid changes in nitrate concentration, and thereby modulate their rate of organ production to the availability of mineral nutrients within a few days. Our work sheds new light on the role of the stem cell regulatory network, by showing that it does not only maintain meristem homeostasis but also allows plants to adapt to rapid changes in the environment.

Plants have evolved specific mechanisms to adapt their growth and physiology to the availability of mineral nutrients in their environment[5]. Various hormones such as auxin, abscisic acid, gibberellin and cytokinins have been shown to act in this process either locally or systemically[5]. Cytokinins in particular play an essential role in plant response to nitrate, where they act as second messengers[6]. For example, cytokinins promote lateral root development in areas rich in NO_3 if the overall NO_3 availability for the plant is low[7]. In the shoot, cytokinins have been shown to modulate key traits such as leaf size[8,9] and branch number[10] in response to nitrate.

Cytokinins have also been shown to be critical for the maintenance of stem cell homeostasis in the SAM. By modulating the expression of *WUSCHEL*, a homeodomain transcription factor expressed in the center of the meristem, cytokinins promote stem cell proliferation, thus controlling the size of the meristem and the rate of shoot organogenesis[11-14]. Using grafting experiments, a recent study showed that a systemic signal of a cytokinin precursor (trans-zeatin-riboside: tZR), travelling from root to shoot through xylem, could influence the size of the vegetative meristem[3]. However, it remains unclear whether cytokinin signalling can allow the SAM to respond to changes in nutrient levels in the environment. Here, we examined how a core stem cell regulator in the SAM dynamically responds to changes in mineral nutrient levels in the soil and whether systemic cytokinin signals can account for the dynamic adaptation of meristem function to nutrient levels. We used the inflorescence meristem of *Arabidopsis* as a model as this structure produces all of the flowers of the plant and is therefore a key target for crop improvement.

46

47　We first studied how fixed levels of nutrients affect meristem function, by growing plants on soil
48　containing different levels of nutrients. To assess meristem function, we measured the size of the
49　meristem, the plastochron ratio (a feature that is inversely proportional to the organogenesis rate of
50　the SAM) and the number of flowers produced by the primary inflorescence (Methods). We
51　observed that bigger, well-nourished plants had larger meristems and produced more flowers than
52　smaller, more poorly nourished plants (Fig. 1a, Supplementary Fig. 1). We found a very close
53　correlation between the weight of the rosette and the size of the meristem in individual plants
54　(Fig.1b), showing that shoot development is coordinated when plants are grown under different
55　nutritional conditions.

56

57　We next examined whether the observed changes in meristem size were linked to changes in stem
58　cell homeostasis, by examining fluorescent reporters for the key meristem regulatory genes, *WUS*
59　and *CLAVATA3* (*CLV3*). We developed a pipeline based on projections of 3D confocal stacks to
60　automatically extract and analyse gene expression domains using a generalized exponential fit
61　function (Methods, Supplementary Fig. 2). The intensity of the signal and the size of the domain of
62　expression of *pWUS::GFP* were strongly correlated with the size of the SAM in the different growth
63　conditions (Fig. 1c, Supplementary Fig. 3a and b), which was also confirmed using a translational
64　fusion (Supplementary Fig. 3c). *CLV3* did not show such behaviour in all experimental repeats and
65　only the size of its expression domain consistently correlated weakly with the size of the SAM
66　(Supplementary Fig. 3d). Such an uncoupling between *WUS* and *CLV3* expression has been described
67　in vegetative meristems under different light levels[15] and suggests that these two genes could be
68　differentially regulated by both nutrients and light.

69

70　As cytokinins modulate *WUS* and *CLV3* expression[11-13], we examined the expression of *pTCSn::GFP*, a
71　reporter of cytokinin response, when plants were grown with different levels of nutrients. Similarly
72　to what was observed with *WUS,* the intensity of the signal and the size of the domain of expression
73　of the *pTCSn::GFP* reporter correlated with the size of the meristem in the different growth
74　conditions (Fig. 1d, Supplementary Fig. 3e and f), thus showing that plants growing with higher levels
75　of nutrients exhibit higher levels of cytokinin signalling in the SAM. As altering cytokinin signalling is
76　known to affect meristem homeostasis[16-21], we further studied the phenotype in the meristem of
77　various mutants of cytokinin metabolism and their response to mineral nutrition.

78　First, we looked at the phenotype of mutants altered in the successive steps of production of
79　cytokinins[22]: *ipt3-1 ipt5-2 ipt7-1* (referred to here as *ipt3.5.7*) for the first step of biosynthesis, *log4-3*
80　*log7-1* (*log4.7*) and *log1-2 log3-2 log4-3 log7-1* (*log1.3.4.7*) for the second step of biosynthesis and
81　for mutants for the conversion of cytokinins[23]: *cyp735a1-1 cyp735a2-1* (*cyp735a1.2*) and the
82　degradation of cytokinins[16]: *ckx3-1 ckx5-2* (*ckx3.5*) in plants grown on soil supplied with fertilizer.
83　Mutant shoots grew almost normally in this condition and only the *ipt3.5.7* and *cyp735a1.2* mutants
84　showed a slight decrease in rosette weight (Fig. 2a and Supplementary Fig. 4a). However, meristem
85　size and organogenesis rate were strongly affected by the mutations (Fig. 2b and c, Supplementary
86　Fig. 4b-d). The *ipt3.5.7*, *log4.7,* *log1.3.4.7* and *cyp735a1.2* mutants, altered in various steps of tZ
87　production, showed smaller inflorescence meristems that produced fewer organs. In contrast, the
88　*ckx3.5* mutant, which displays higher levels of cytokinins, showed larger inflorescence meristems
89　that produced more organs, as previously described[16]. We also quantified the size of the domain of

90   expression of *WUS* by *in situ* hybridization (Supplementary Fig. 4e). We observed changes in the size

91   of the *WUS* expression domain in all genotypes that correlated with the changes in meristem size we

92   quantified, thus supporting the idea that cytokinin metabolism controls meristem function through

93   the stem cell regulatory network.

94   We next looked at the effect of mineral nutrition on the phenotype of the mutants by comparing

95   plants grown on soil with or without fertilizer. Of all mutants, only *ipt3.5.7* mutants did not respond

96   to fertilizer with an increase in meristem size and organogenesis rate, as observed in WT. Instead, it

97   displayed a surprising statistically significant decrease in meristem size (Fig. 2b and c). Although all

98   the enzymes involved in cytokinin metabolism can modulate meristem homeostasis, *ISOPENTENYL-*

99   *TRANSFERASE* enzymes *(IPT)*, which catalyse the first step of cytokinin production, appear to be the

100   only ones necessary for the response of the meristem to changes in nutrient availability in the soil.

101   This result is supported by the fact that nitrate, the main mineral nutrient, can directly modulate the

102   expression of *IPT3* and to a lesser extent of *IPT5* in seedlings[24]. To further support that the response

103   of meristems to mineral nutrients relies on cytokinin precursors produced by *IPT* enzymes, we used

104   mass spectrometry to compare CK levels in inflorescences of plants grown without or with fertilizer.

105   Despite technical variability in the mass spectrometry measurements, we observed a statistically

106   significant increase in the levels of tZR precursors, the dephosphorylated products of *IPT* enzymes, in

107   the two experimental replicates, further supporting the importance of these enzymes in the

108   response of the meristem to nutrients (Supplementary Fig. 5f). We did not find significant changes in

109   the levels of the active cytokinin tZ in the whole inflorescence but found a significant increase in the

110   levels of the degradation products of tZ: tZROG (trans-zeatin ribose-O-glucose) and tZ7G (trans-

111   zeatin-7-glucose). The lack of changes in tZ levels could be a result of tZ being a transient molecule

112   mainly synthesized locally in the meristem, notably through the action of LOG4 and LOG7 enzymes[11-

113   13].

114   We further studied the spatial origin of the signal triggering the response of the meristem to mineral

115   nutrition. Grafting experiments have previously shown that cytokinins can act either as local or as

116   systemic signals in the control of root and shoot development[3,23,25]. We performed grafting

117   experiments on our set of mutants to study whether a systemic signal is involved in the control of

118   meristem function. Adding a WT root was able to rescue the phenotype in the meristem of *ipt3.5.7*

119   and *cyp735a1.2* mutants but not of the *ckx3.5* and of the two *log* mutants (Fig. 3a and b,

120   Supplementary Fig. 5a). Grafting a mutant root onto a WT scion led to a minor but statistically

121   significant decrease in meristem size for *log1.3.4.7*, *ipt3.5.7* and *cyp735a1.2* mutant roots

122   (Supplementary Fig. 5b-d). These experiments show that expressing *IPT* and *CYP735A* in either part

123   of the plant is sufficient but not completely necessary for proper meristem function, but that *LOG*

124   and *CKX* must act largely in the shoot to regulate meristem function. Our results are in agreement

125   with the recent work by Osugi and colleagues, who showed that the phenotype in the vegetative

126   meristem of the *ipt* triple mutant but not the *log* sextuple mutant could be complemented by

127   grafting a WT root[3]. These results also make sense in light of the expression patterns of the different

128   genes, as *LOG* and *CKX* enzymes are expressed in meristems[11,13,16], while *IPTs* and *CYP735*a1-2 are

129   expressed predominantly in the vascular tissues of the root and to a lesser extent of the shoot[19,26] -

130   only *IPT7* expression has been shown to be induced by *STM* in the vegetative meristem[27].

131   To analyse the dynamics between production of cytokinin precursors and modulation of meristem

132   function, we applied tZR and tZ to meristems expressing *pTCSn::GFP* and *pWUS::GFP* cut from the

133   plant and grown *in vitro* (see Methods). In the absence of added cytokinin, both *pTCSn::GFP* and

134   *pWUS::GFP* signal strongly decreased over a 48h time course, suggesting that extrinsic cytokinin is

135   needed to sustain meristem homeostasis. In contrast, adding 50 µM either of tZR or tZ to the

136   medium upregulated *pTCSn::GFP* expression ectopically and allowed the maintenance of the

137   *pWUS::GFP* signal in the centre of the meristem (Fig. 3c and d). Inducing *IPT3* in cut meristems in the

138   absence of extrinsic cytokinin also maintained, at least partially, *WUS* expression (Supplementary

139   Fig. 6). Together with the results from the grafting experiments, these data support a model where

140   stem cell homeostasis is controlled by a systemic signal of cytokinin precursors (tZR) produced by *IPT*

141   enzymes outside of the meristem, which are locally converted to active cytokinins by *LOG* enzymes

142   in the shoot meristem.

143

144   Adding nitrate (NO_3) to nitrogen-deficient plants leads to a rapid increase in cytokinin levels in the

145   plant[3,24,28,29]. Given the rapid response of meristems to changes in cytokinin levels we observed *in*

146   *vitro*, we looked to see if the meristem could dynamically respond to changes in nitrate

147   concentration *in vivo.* We grew plants on sand, watering them with a nutritive solution containing a

148   low concentration of nitrate (1.8 mM of NO_3 as the only source of nitrogen) to induce a deficiency[10].

149   Once the plants bolted, we watered them with a nutritive solution containing different

150   concentrations of NO_3 (0 mM, 1.8 mM or 9mM) and quantitatively analysed the dynamics of

151   response to this treatment. In the SAM, the treatment led to the dose-dependent induction of

152   *pTCSn::GFP* and of *pWUS::GFP* expression within only one day and to an increase of meristem size

153   and of the organogenesis rate within 2 to 3 days (Fig. 4a-c, Supplementary Fig. 7). We then checked

154   whether this response relied on changes in cytokinin levels in the plant. In the root, we confirmed

155   that the addition of nitrate to deficient plants led to a rapid, dose-dependent and transient induction

156   of nitrate signalling (inferred from the level of expression of the nitrate responsive gene *NIA1*) and of

157   *IPT3* and *5* (Supplementary Fig. 8a). By measuring the levels of cytokinin species by mass

158   spectrometry, we also confirmed that the treatment led to a significant increase in the

159   concentration of cytokinin precursors (tZR and/or tZRP depending on the tissues) and products of

160   degradation (tZ7G, tZ9G, and/or tZROG depending on the tissues, Supplementary Fig. 8b). Finally, we

161   analysed the meristem response in our set of mutants, three days after a nitrate treatment (9 mM

162   NO_3). Similar to what we observed on plants grown in soil, the response of *ipt3.5.7* mutant plants to

163   nitrate in the meristem was strongly reduced, though statistically significant in one of the two

164   experimental repeats, while response in the other mutant backgrounds was as in wild type (Fig. 4d,

165   supplementary Fig. 9). In summary, our data show that the addition of nutrients leads to a response

166   of the stem cell regulatory network within a day and that the rapid changes in meristem properties

167   can be explained by the same cytokinin-based mechanism of signal propagation as we found for

168   different fixed nutrient conditions (Fig. 2).

169

170   Taken together, our results show that the meristem can adapt the rate of shoot organogenesis to

171   the availability of nitrate in the soil. Mechanistically, this phenomenon correlates with the ability of

172   *WUS* to quantitatively respond to changes in the concentration of cytokinin precursors produced in

173   the plant in response to variations in nitrate levels. As the main inflorescence of WT plants growing

174   on soil only produced an average of 3.1 ± 0.4 flowers per day (n=16), the response of the SAM to

175   changes in nitrate levels, which leads to significant changes in the rate of organ production in only

176   two days, should be seen as very rapid in comparison to the pace of morphogenesis in this tissue.

177   The timing of the response to nutrients is very similar to the response to induced perturbations of

178 the core network[30], in both cases causing expression domain changes in a day followed by changes in
179 growth and size. Our findings thus expand the understanding of the function of the stem cell
180 regulatory network in the SAM. They show that this network not only acts to maintain the integrity
181 of the SAM during organogenesis, but also allows a very rapid adaptation of SAM function to a
182 nutritional cue.
183
184 A recent study showed that vegetative meristems of seedlings germinating in the dark displayed
185 reduced *WUS* expression, which was controlled by the activity of *CKX* enzymes[15]. Given the
186 pleiotropic effects of cytokinins[6], we can hypothesize that different environmental signals could be
187 integrated through cytokinin signalling, and lead to different developmental responses in the
188 meristem depending on whether they modulate, locally or globally, different aspects of cytokinin
189 signalling.
190
191 Although it was developed in *Arabidopsis*, this model can in future be applied to crops, where
192 cytokinin metabolism and action on stem cell regulation should be conserved. In rice, where *LOG*
193 mutants were first characterized[18], quantitative trait loci (QTL) for increased grain productivity have
194 been mapped to genes involved in the regulation of cytokinins, including notably a CKX enzyme-
195 encoding gene[31,32]. In maize, weak mutants of *FASCIATED-EAR3*, a receptor able to bind a *CLV3*
196 homolog and involved in the control of *WUS* expression, also shows increased seed yield[33]. Our
197 work, which provides a novel and integrative model based on nutrient availability, cytokinin
198 metabolism and its effect on stem cell regulation and meristem function (Supplementary Fig. 10),
199 allows a better characterization of the influence of mineral nutrients on plant architecture and could
200 be used to better understand plant response to environmental inputs, and to develop new cultivars
201 with increased yield.
202

203 **Author Contributions:**
204 B.L., C.W.M., E.M.M., J.C.W.L. and H.J. designed the experiments. B.L., A.M., C.W.M., C.S., W.Y.
205 performed the experiments. B.L., P.F.-J., A.M., C.S. and C.T. analysed the data. B.L., E.M.M., J.C.W.L.
206 and H.J. wrote the paper with inputs from all co-authors.
207

218

219 **Competing interests:**
220 The authors declare the absence of any competing interest.
221

222 1 Barton, M. K. Twenty years on: the inner workings of the shoot apical meristem, a
223   developmental dynamo. *Dev Biol* **341**, 95-113, doi:10.1016/j.ydbio.2009.11.029 (2010).
224 2 Pfeiffer, A., Wenzl, C. & Lohmann, J. U. Beyond flexibility: controlling stem cells in an ever
225   changing environment. *Curr Opin Plant Biol* **35**, 117-123, doi:10.1016/j.pbi.2016.11.014
226   (2017).
227 3 Osugi, A. *et al.* Systemic transport of trans-zeatin and its precursor have differing roles in
228   Arabidopsis shoots. *Nat Plants* **3**, 17112, doi:10.1038/nplants.2017.112 (2017).
229 4 Laux, T., Mayer, K. F., Berger, J. & Jurgens, G. The WUSCHEL gene is required for shoot and
230   floral meristem integrity in Arabidopsis. *Development* **122**, 87-96 (1996).
231 5 Krouk, G. *et al.* A framework integrating plant growth with hormones and nutrients. *Trends*
232   *Plant Sci* **16**, 178-182, doi:10.1016/j.tplants.2011.02.004 (2011).
233 6 Werner, T. & Schmulling, T. Cytokinin action in plant development. *Curr Opin Plant Biol* **12**,
234   527-538, doi:10.1016/j.pbi.2009.07.002 (2009).
235 7 Ruffel, S. *et al.* Nitrogen economics of root foraging: transitive closure of the nitrate-
236   cytokinin relay and distinct systemic signaling for N supply vs. demand. *Proc Natl Acad Sci U*
237   *S A* **108**, 18524-18529, doi:10.1073/pnas.1108684108 (2011).
238 8 Rahayu, Y. S. *et al.* Root-derived cytokinins as long-distance signals for NO3--induced
239   stimulation of leaf growth. *J Exp Bot* **56**, 1143-1152, doi:10.1093/jxb/eri107 (2005).
240 9 Walch-Liu, P., Neumann, G., Bangerth, F. & Engels, C. Rapid effects of nitrogen form on leaf
241   morphogenesis in tobacco. *J Exp Bot* **51**, 227-237 (2000).
242 10 Muller, D. *et al.* Cytokinin is required for escape but not release from auxin mediated apical
243   dominance. *Plant J* **82**, 874-886, doi:10.1111/tpj.12862 (2015).
244 11 Chickarmane, V. S., Gordon, S. P., Tarr, P. T., Heisler, M. G. & Meyerowitz, E. M. Cytokinin
245   signaling as a positional cue for patterning the apical-basal axis of the growing Arabidopsis
246   shoot meristem. *Proc Natl Acad Sci U S A* **109**, 4002-4007, doi:10.1073/pnas.1200636109
247   (2012).
248 12 Gordon, S. P., Chickarmane, V. S., Ohno, C. & Meyerowitz, E. M. Multiple feedback loops
249   through cytokinin signaling control stem cell number within the Arabidopsis shoot meristem.
250   *Proc Natl Acad Sci U S A* **106**, 16529-16534, doi:10.1073/pnas.0908122106 (2009).
251 13 Gruel, J. *et al.* An epidermis-driven mechanism positions and scales stem cell niches in
252   plants. *Sci Adv* **2**, e1500989, doi:10.1126/sciadv.1500989 (2016).
253 14 Landrein, B. *et al.* Meristem size contributes to the robustness of phyllotaxis in Arabidopsis. *J*
254   *Exp Bot* **66**, 1317-1324, doi:10.1093/jxb/eru482 (2015).
255 15 Pfeiffer, A. *et al.* Integration of light and metabolic signals for stem cell activation at the
256   shoot apical meristem. *Elife* **5**, doi:10.7554/eLife.17023 (2016).
257 16 Bartrina, I., Otto, E., Strnad, M., Werner, T. & Schmulling, T. Cytokinin regulates the activity
258   of reproductive meristems, flower organ size, ovule formation, and thus seed yield in
259   Arabidopsis thaliana. *Plant Cell* **23**, 69-80, doi:10.1105/tpc.110.079079 (2011).
260 17 Higuchi, M. *et al.* In planta functions of the Arabidopsis cytokinin receptor family. *Proc Natl*
261   *Acad Sci U S A* **101**, 8821-8826, doi:10.1073/pnas.0402887101 (2004).
262 18 Kurakawa, T. *et al.* Direct control of shoot meristem activity by a cytokinin-activating
263   enzyme. *Nature* **445**, 652-655, doi:10.1038/nature05504 (2007).
264 19 Miyawaki, K. *et al.* Roles of Arabidopsis ATP/ADP isopentenyltransferases and tRNA
265   isopentenyltransferases in cytokinin biosynthesis. *Proc Natl Acad Sci U S A* **103**, 16598-
266   16603, doi:10.1073/pnas.0603522103 (2006).
267 20 Nishiyama, R. *et al.* Analysis of cytokinin mutants and regulation of cytokinin metabolic
268   genes reveals important regulatory roles of cytokinins in drought, salt and abscisic acid
269   responses, and abscisic acid biosynthesis. *Plant Cell* **23**, 2169-2183,
270   doi:10.1105/tpc.111.087395 (2011).

271   21   Werner, T. *et al.* Cytokinin-deficient transgenic Arabidopsis plants show multiple
272   developmental alterations indicating opposite functions of cytokinins in the regulation of
273   shoot and root meristem activity. *Plant Cell* **15**, 2532-2550, doi:10.1105/tpc.014928 (2003).
274   22   Kieber, J. J. & Schaller, G. E. Cytokinins. *Arabidopsis Book* **12**, e0168, doi:10.1199/tab.0168
275   (2014).
276   23   Kiba, T., Takei, K., Kojima, M. & Sakakibara, H. Side-chain modification of cytokinins controls
277   shoot growth in Arabidopsis. *Dev Cell* **27**, 452-461, doi:10.1016/j.devcel.2013.10.004 (2013).
278   24   Takei, K. *et al.* AtIPT3 is a key determinant of nitrate-dependent cytokinin biosynthesis in
279   Arabidopsis. *Plant Cell Physiol* **45**, 1053-1062, doi:10.1093/pcp/pch119 (2004).
280   25   Matsumoto-Kitano, M. *et al.* Cytokinins are central regulators of cambial activity. *Proc Natl
281   Acad Sci U S A* **105**, 20027-20031, doi:10.1073/pnas.0805619105 (2008).
282   26   Miyawaki, K., Matsumoto-Kitano, M. & Kakimoto, T. Expression of cytokinin biosynthetic
283   isopentenyltransferase genes in Arabidopsis: tissue specificity and regulation by auxin,
284   cytokinin, and nitrate. *Plant J* **37**, 128-138 (2004).
285   27   Yanai, O. *et al.* Arabidopsis KNOXI proteins activate cytokinin biosynthesis. *Curr Biol* **15**,
286   1566-1571, doi:10.1016/j.cub.2005.07.060 (2005).
287   28   Takei, K., Sakakibara, H., Taniguchi, M. & Sugiyama, T. Nitrogen-dependent accumulation of
288   cytokinins in root and the translocation to leaf: implication of cytokinin species that induces
289   gene expression of maize response regulator. *Plant Cell Physiol* **42**, 85-93 (2001).
290   29   Peterson, J. B. & Miller, C. O. Cytokinins in Vinca rosea L. Crown Gall Tumor Tissue as
291   Influenced by Compounds Containing Reduced Nitrogen. *Plant Physiol* **57**, 393-399 (1976).
292   30   Reddy, G. V. & Meyerowitz, E. M. Stem-cell homeostasis and growth dynamics can be
293   uncoupled in the Arabidopsis shoot apex. *Science* **310**, 663-667,
294   doi:10.1126/science.1116261 (2005).
295   31   Ashikari, M. *et al.* Cytokinin oxidase regulates rice grain production. *Science* **309**, 741-745,
296   doi:10.1126/science.1113373 (2005).
297   32   Wu, Y. *et al.* The QTL GNP1 Encodes GA20ox1, Which Increases Grain Number and Yield by
298   Increasing Cytokinin Activity in Rice Panicle Meristems. *PLoS Genet* **12**, e1006386,
299   doi:10.1371/journal.pgen.1006386 (2016).
300   33   Je, B. I. *et al.* Signaling from maize organ primordia via FASCIATED EAR3 regulates stem cell
301   proliferation and yield traits. *Nat Genet* **48**, 785-791, doi:10.1038/ng.3567 (2016).

302

Main figures:

Fig. 1 Plant nutritional status influences shoot meristem homeostasis.
a. Morphology of the rosette (top, scale bar: 1 cm) and of the SAM (bottom, scale bar: 50 μm) of representative WT plants grown on soils of different nutritive quality. b. Correlation between rosette weight and SAM size of WT plants grown on soils of different nutritive quality (n=109, pool of 2 independent experiments). c. and d. *pWUS::GFP* (c) and *pTCSn::GFP* (d) expression in WT plants grown on soils of different nutritive quality (scale bars: 50 μm, n=55 (c) and n=57 (d)). Top panels show representative plants. Red arrows point to the center of the inflorescence meristem. The lower panels show total fluorescent signal (Methods) in the inflorescence meristem vs. meristem size. Data were fitted using linear models.

Fig. 2 Cytokinins allow the adaptation of meristem function to plant nutritional status
a. Morphology of the rosette (top, scale bar: 1 cm) and of the SAM (bottom, scale bar: 50 μm) of representative WT and CK-associated mutant plants. b. and c. Meristem size (b) and plastochron ratio (c) of WT and CK-associated mutant plants grown on soil without (green, g) or with fertilizer (red, r) (Col-0: n= 22 (g) and 25 (r), *ckx3.5*: n= 23 (g) and 27 (r), *log4.7*: n= 19 (g) and 24 (r), *log1.3.4.7*: n= 14 (g) and 25 (r), *ipt3.5.7*: n= 36 (g) and 20 (r), *cyp735a1.2*: n= 26 (g) and 20 (r), pool of 2 independent experiments). Data were compared using Student's t-test.
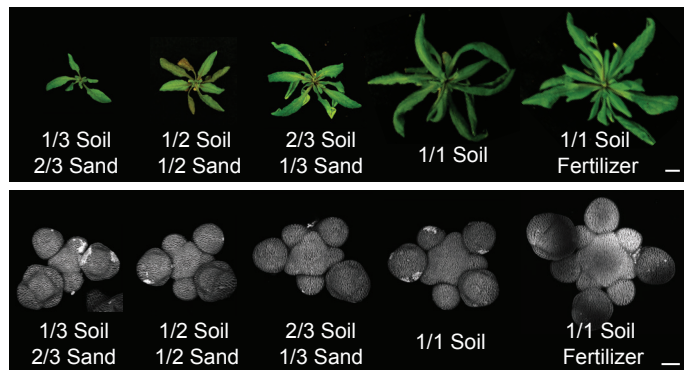
Fig. 3 Cytokinin precursors act as long-range signals in the control of SAM homeostasis
a. Representative meristems of WT and cytokinin-associated mutant plants self-grafted or grafted with a WT rootstock and grown on soil supplied with fertilizer (Scale bar: 50 μm). b. Meristem size of WT and cytokinin-associated mutant plants self-grafted or grafted with a WT rootstock and grown on soil supplied with fertilizer (pools of two independent experiments, the numbers of replicates are displayed in the figure). Data were compared using Student's t-tests. c. and d. Effect of tZR and tZ application on the expression of *pTCSn::GFP* (c) and *pWUS::GFP* (d) in cut meristems grown *in vitro* (scale bars: 50 μm, pools of two independent experiments, *pTCSn::*GFP: n=11 for each condition, *pWUS::GFP*: n=12 for each condition). Top panels show representative plants. Red arrows point to the center of the inflorescence meristem. Lower panels show total florescent signal in the inflorescence meristem (Methods). Data were compared using Student's t-test.
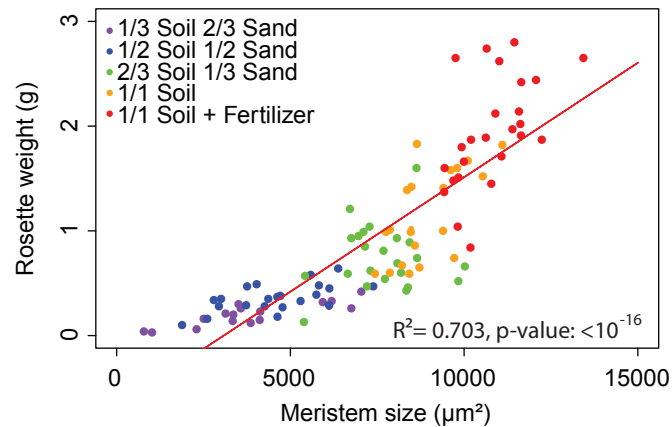
Fig. 4 Nitrate modulates meristem homeostasis through *IPTs*
a. to c. Effect of nitrate resupply on *pTCSn::GFP* expression (a), *pWUS::GFP* expression (b), and meristem size and plastochron ratio (c). The treatment was performed at day 0 and different meristems were dissected and imaged each day (Scale bars: 50 μm, n=8 to 12). (a and b) Left panels show representative plants, and right panels show quantification of total florescent signal (Methods). Red arrows point to the center of the inflorescence meristem. Data were compared using Student's t-test. d. Meristem size and plastochron ratio of WT and cytokinin-associated mutants three days after treatment with a nutritive solution containing either 0 mM (green, g) or 9 mM of NO_3 (red, r) (Col-0: n= 21 (g) and 24 (r), *ckx3.5*: n= 13 (g) and 12 (r), *log4.7*: n= 17 (g) and 18 (r), *log1.3.4.7*: n= 13 (g) and 15 (r), *ipt3.5.7*: n= 18 (g) and 19 (r), *cyp735a1.2*: n= 14 (g) and 14 (r)). Data were compared using Student's t-test.
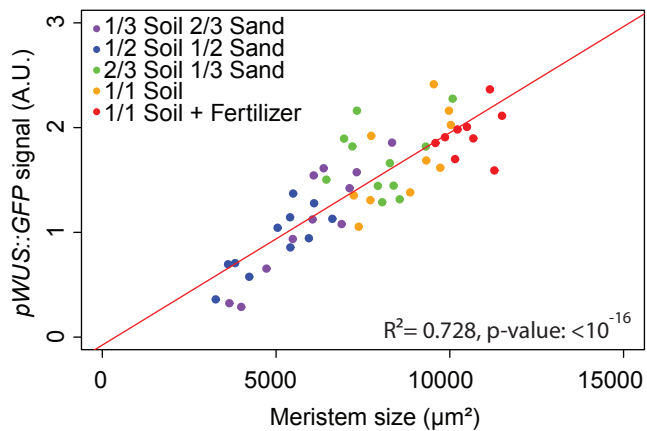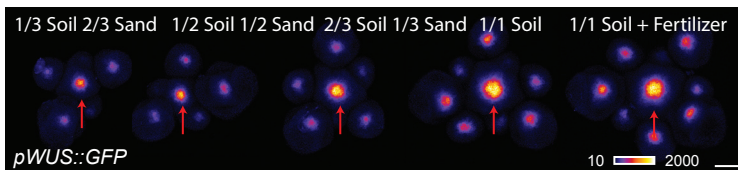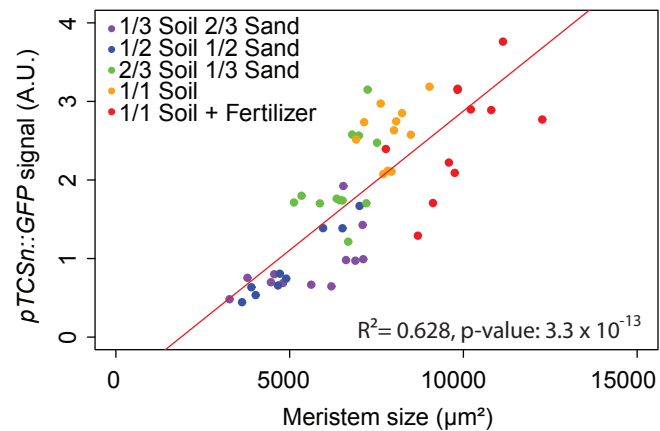
a

1/3 Soil 2/3 Sand | 1/2 Soil 1/2 Sand | 2/3 Soil 1/3 Sand | 1/1 Soil | 1/1 Soil Fertilizer

1/3 Soil 2/3 Sand | 1/2 Soil 1/2 Sand | 2/3 Soil 1/3 Sand | 1/1 Soil | 1/1 Soil Fertilizer

b

- 1/3 Soil 2/3 Sand
- 1/2 Soil 1/2 Sand
- 2/3 Soil 1/3 Sand
- 1/1 Soil
- 1/1 Soil + Fertilizer

Rosette weight (g)

Meristem size (µm²)

$R^2 = 0.703$, p-value: $<10^{-16}$

c

1/3 Soil 2/3 Sand | 1/2 Soil 1/2 Sand | 2/3 Soil 1/3 Sand | 1/1 Soil | 1/1 Soil + Fertilizer

pWUS::GFP

10 ▮▮▮ 2000

- 1/3 Soil 2/3 Sand
- 1/2 Soil 1/2 Sand
- 2/3 Soil 1/3 Sand
- 1/1 Soil
- 1/1 Soil + Fertilizer

pWUS::GFP signal (A.U.)

Meristem size (µm²)

$R^2 = 0.728$, p-value: $<10^{-16}$

d

1/3 Soil 2/3 Sand | 1/2 Soil 1/2 Sand | 2/3 Soil 1/3 Sand | 1/1 Soil | 1/1 Soil + Fertilizer

pTCSn::GFP

200 ▮▮▮ 2000

- 1/3 Soil 2/3 Sand
- 1/2 Soil 1/2 Sand
- 2/3 Soil 1/3 Sand
- 1/1 Soil
- 1/1 Soil + Fertilizer

pTCSn::GFP signal (A.U.)

Meristem size (µm²)

$R^2 = 0.628$, p-value: 3.3×10^{-13}

a

1/1 Soil + Fertilizer

Col-0   ckx3.5   log4.7   log1.3.4.7   ipt3.5.7   cyp735a1.2

1/1 Soil + Fertilizer

Col-0   ckx3.5   log4.7   log1.3.4.7   ipt3.5.7   cyp735a1.2

b

Meristem size (µm²)

■ 1/1 Soil
■ 1/1 Soil + Fertilizer

p<0.001
p<0.001
p<0.001
p<0.001
p<0.001
p<0.001

Col-0   ckx3.5   log4.7   log1.3.4.7   ipt3.5.7   cyp735a1.2

c

Plastochron ratio

■ 1/1 Soil
■ 1/1 Soil + Fertilizer

p<0.001
p<0.001
p=0.018
p=0.004
p=0.088
p<0.001

Col-0   ckx3.5   log4.7   log1.3.4.7   ipt3.5.7   cyp735a1.2

a

ckx3.5 / *ckx3.5*	*log4.7* / *log4.7*	*log1.3.4.7* / *log1.3.4.7*	*ip3.5.7* / *ipt3.5.7*	*cyp735a1.2* / *cyp735a1.2*
Col-0 / Col-0				
ckx3.5 / Col-0	*log4.7* / Col-0	*log1.3.4.7* / Col-0	*ip3.5.7* / Col-0	*cyp735a1.2* / Col-0

b

Rootstock: Col-0 (green), mutant (red)

Meristem size (μm²)

Col-0	*ckx3.5* p=0.248	*log4.7* p=0.026	*log1.3.4.7* p=0.759	*ipt3.5.7* p<0.001	*cyp735a1.2* p<0.001
n=115	n=41, n=35	n=35, n=32	n=37, n=35	n=58, n=49	n=26, n=27

Genotype of the scion

c *pTCSn::GFP*

Control / 50μM tZR / 50μM tZ (t0h, t24h, t48h)

pTCSn::GFP signal (normalized by signal at t0h)

Legend: Control (green), 50μM tZR (orange), 50μM tZ (red)

t24h: p<0.001, p<0.001
t48h: p<0.001, p<0.001

d *pWUS::GFP*

Control / 50μM tZR / 50μM tZ (t0h, t24h, t48h)

pWUS::GFP signal (normalized by signal at t0h)

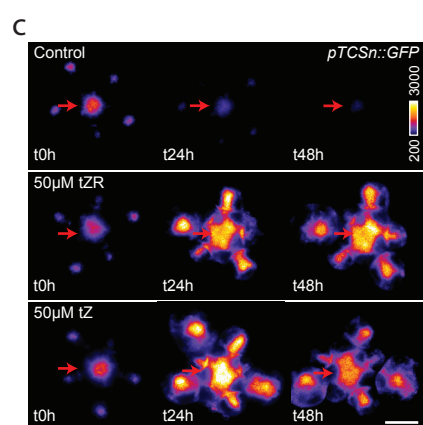Legend: Control (green), 50μM tZR (orange), 50μM tZ (red)
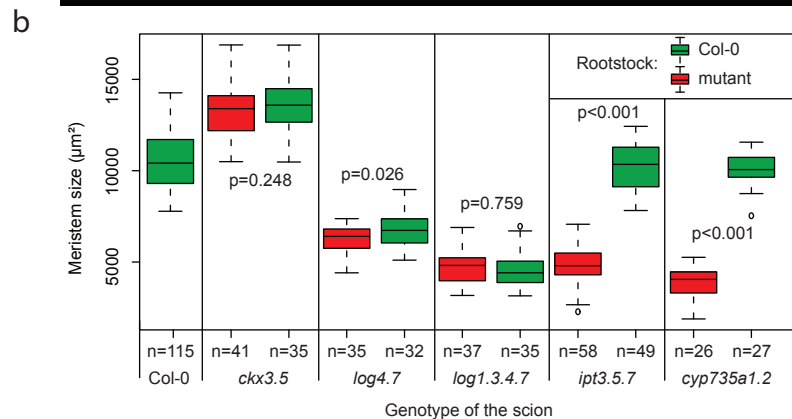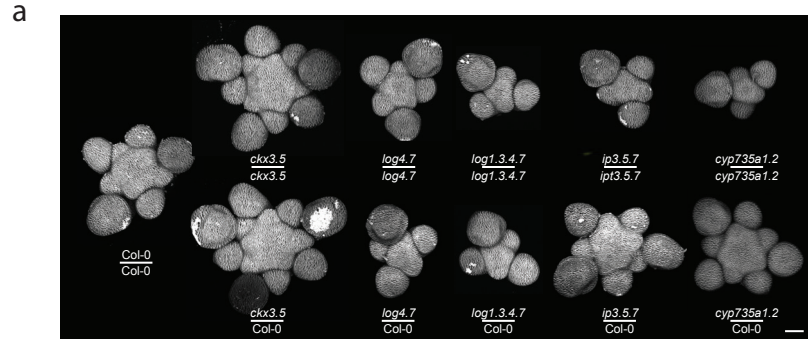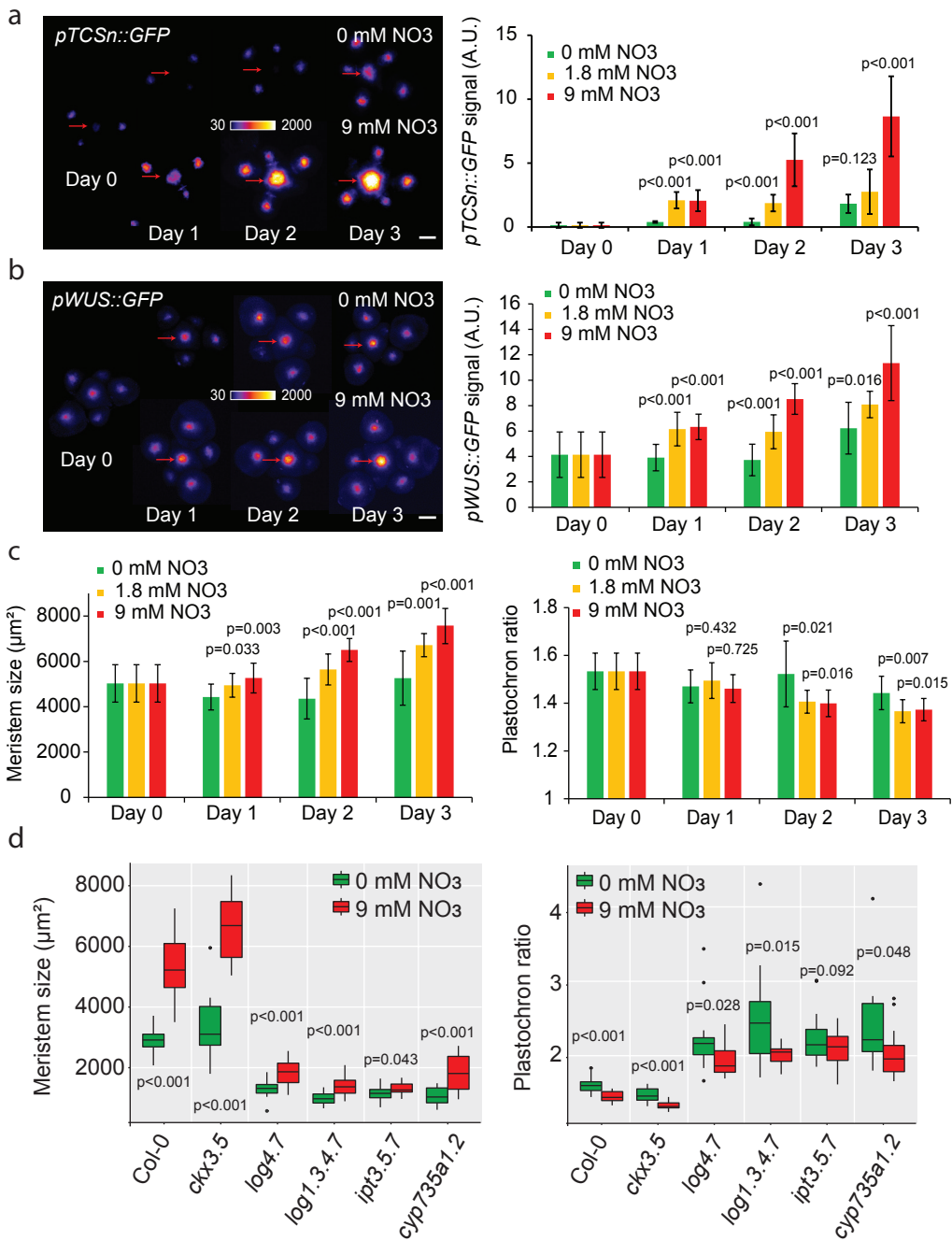
t24h: p<0.001, p<0.001
t48h: p<0.001, p<0.001

1 **Methods:**

2 **Plant Materials:**

3 Col-0 seeds were provided by the Salk stock center. The *pCLV3::dsRED* and *pWUS::GFP* marker lines

4 were previously described[1,2]. The *pTCS::GFP* marker was provided by Teva Vernoux[3] and the

5 *pTCSn::GFP* was provided by Bruno Müller[4].The *WUS-GFP* marker complementing the *wus* mutant

6 phenotype was kindly provided by Jan Lohmann[5]. The triple *ipt* mutant *ipt3-1; ipt5-2; ipt7-1* (*ipt3.5.7*)

7 was provided by Ottoline Leyser[6]. The *log4-3; log7-1* (*log4.7*), *log1-2; log3-2; log4-3; log7-1* (*log1.3.4.7*)

8 and *cyp735a1-1; cyp735a2-1 (cyp735a1.2)* mutant seeds were kindly provided by Hitoshi Sakakibara

9 and the RIKEN Institute[7]. The *ckx3-1* (SAIL_55_G12/CS870580); *ckx5-2* (Salk_117512C) double mutant

10 has already been described[8] and was generated by Paul Tarr.

11 **Growth conditions:**

12 For all plants grown on soil, batches of seeds were dispersed in pots of soil (Levington F2) and placed

13 for 3 days in a 4°C room for stratification and then 7 days in a short day room (8h light) for germination.

14 Seedlings were transferred in to separate pots containing different mixes of sand (Royal Horticultural

15 Society: Silver Sand) and soil (Levington F2) and put into a constant light room (24 h light, temperature:

16 22°C, light intensity 160 µmol $m^{-2} s^{-1}$). Plants were watered without or with 1/1/1 fertilizer (Vitafeed

17 Standard). The experiments were carried out at the beginning of the flowering stage when the main

18 inflorescence stem was of few centimetres in height.

19 For the nitrate resupply experiment, seedlings were germinated on soil and put in a short day room

20 (8h light) for 7 days after stratification before being transferred into small individual pots of ½ sand

21 (Leighton Buzzard sand from WBB Minerals) ½ Terra-green (Oil-Dri) pre-watered with 25 mL of an ATS-

22 derived (*Arabidopsis* salts medium) nutritive solution containing 1.8 mM of NO_3 prepared by adjusting

23 the concentrations of the following components: 0.4 mM $Ca(NO_3)_2$, 1 mM KNO_3, 4 mM KCl and 1.6

24 mM $CaCl_2$[9,10]. Plants were put for 2 weeks in a short day room (8h light) before being transferred into

25 a constant light room. Each plant was fed weekly with 10 mL of the same nutrient solution. The

26 experiments were carried out at the beginning of the flowering stage when the main inflorescence

27 stem was of few centimetres in height. At the beginning of the experiment (at day 0), plants were

28 randomized, separated into three populations and watered with 25 mL of the nutritive solution

29 containing either 0 mM of NO_3 (by adjusting the concentrations of the following components: 0 mM

30 $Ca(NO_3)_2$, 0 mM KNO_3, 5 mM KCl and 2 mM $CaCl_2$), 1.8 mM of NO_3 (same solution as described earlier)

31 or 9 mM of NO_3 (normal ATS solution). Each day, 5-10 plants were used for analysis.

32

33 Within the course of the experiments, we realized that the tap water used for watering the plants

34 contained non-negligible levels of NO_3 (up to 0.7 mM in the summer), which could have moderately

35 influenced our measurements and explain some of the differences observed between experimental

36 repeats. Note however that within an experimental repeat, all genotypes or conditions were grown

37 simultaneously and experienced the same growth conditions.

38

39 **Generation of the *p35S::XVE-IPT3-TFP* line:**

40 The coding sequence of *IPT3* was amplified from Col-0 cDNA (primers: F:

41 TTTGGATCCTATGATCATGAAGATATCT-ATGGCTATG and R: AATGAATTCTCGCCACT-AGACACCGCGAC)

42 and put by conventional cloning into a pENTR1Ad modified vector containing a synthetic sequence for

43 a GS repeat linker peptide of 30 amino acids identical to the one described in[5]. Then, a LR

44   recombination was performed using the *p35S::XVE-pENTR-R4-L1* plasmid described in[11] and kindly

45   provided by Ari-Pekka Mähönen, the *pENTR1Ad-IPT3-linker*, *TFP-pENTR-R2-L3* (Turquoise fluorescent

46   protein) and the *pH7m34GW* destination vector coding for hygromycine resistance. The resulting

47   plasmid was transformed into *Arabidopsis* plants carrying either both *pTCS::GFP* and *pCLV3::dsRED* or

48   *pWUS::GFP* by flower dip transformation. Although we could see the effect of inducing *IPT3-TFP* in

49   multiple independent insertions for each marker, we could only observe a very weak TFP signal by

50   confocal microscopy.

51

52   **Image acquisition and time-lapse:**

53   Imaging was performed as follows: First, the main inflorescence meristem of plants at the beginning

54   of the flowering stage was cut one to two centimetres from the tip, dissected under a binocular

55   stereoscopic microscope to remove all the flowers older than stage 3 (as defined in[12]) and transferred

56   to a box containing an apex culture medium (ACM) with vitamins as described in[13]. Meristems were

57   imaged in water using a 20X long-distance water-dipping objective mounted either on a LSM700 or a

58   LSM780 confocal microscope (Zeiss, Germany). Z-stacks of 1 or 2 µm spacing were taken. In some

59   experiments, meristems were put in contact with a solution of 0.1 mg/mL of FM4-64 (Thermo-Fisher)

60   for 10 minutes prior to imaging to dye the cell membranes. For the time-lapse experiment looking at

61   the effect of extrinsic cytokinin, meristems were put in a box of ACM with vitamins and without or

62   with 50µM of tZR or of tZ (Sigma) diluted from 50mM stock solutions. To prepare those stock solutions,

63   tZR was dissolved in 10mM NaOH and tZ in DMSO. Meristems were kept in a constant light phytotron

64   and covered with the same solution of liquid ACM for imaging. For the time-lapse experiment looking

65   at the effect of an estradiol-based induction of *IPT3*, meristems were put in a box of ACM with vitamins

66   and with 5 µM of β-estradiol (Sigma) or with the equivalent volume of DMSO as a control. Again,

67   meristems were kept in a constant light phytotron and covered with the same liquid ACM solution for

68   imaging.

69   **Image Analysis:**

70   Confocal stacks were analysed using the ImageJ software (https://fiji.sc/). Z-projections (maximum

71   intensity) of the stacks were performed to analyse meristems dyed with FM4-64. Z-projections (sum

72   slices) of the stacks were performed to analyse meristems expressing *GFP* or its derivatives and the

73   "fire" lookup table was used to represent the signal. Meristem size and plastochron ratio were

74   measured as described in[14]. Note that as the plastochron ratio is the average area between successive

75   primordia, this parameter is more variable for meristems producing few organs as it is averaged on a

76   smaller number of measurements. The expression level of *pTCSn::GFP* and the expression level and

77   domain size of the *pWUS::GFP*, *WUS-GFP* and *pCLV3::dsRED* were analysed using a Matlab pipeline

78   (Mathworks Inc., Natick, MA) specifically developed for this study (see below).

79   **Characterization of gene expression domains through automated image analysis:**

80   In order to characterize quantitatively the *WUS-GFP*, *pWUS::GFP*, *pTCSn::GFP* and *pCLV3::dsRED*

81   domains in meristems, we developed an automatic pipeline with custom-made code written in

82   Matlab. The code performs two basic tasks: first of all, it automatically identifies the fluorescent

83   domain in the inflorescence meristem. Second, it computes the size and the intensity of such a

84   domain. The domain identification is performed on Gaussian filtered (σ=5µm) maximal intensity

85   projection of the fluorescence image under study, while the size and intensity of the domain

86   calculation is performed on a Gaussian filtered (σ=5µm) sum slices projection. In both tasks, the

87   Gaussian filter is used to smooth out the fluorescence images so that we neutralize the intracellular

88   localization (ER or nucleus) of the fluorescent markers. This produces a more continuous fluorescence
89   domain, which facilitates the automated extraction of its main features. Below, we explain in further
90   detail how this pipeline was structured and used.

91   The automatically identification of the center of *WUS* and *CLV3* expression domains is performed
92   through an Otsu thresholding over the corresponding z-projected and Gaussian-filtered fluorescence
93   images. As floral primordia also express the reporters, it is assumed that the expression domain of the
94   inflorescence meristem is the one that is the closest to the center of each image. Then, the centroid,
95   r_0, of this domain is found and a circular region R of radius ρ_R=40 μm is defined that should contain
96   the fluorescence domain under study in the meristem. In the cases where the expression domain has
97   failed to be automatically detected – e.g., in those images where the meristem was not well centered
98   – we have manually specified the center of the inflorescence meristem.

99   After domain detection, the size of fluorescence domains is determined. To do so, the radially
100   symmetric decay of the fluorescence in the R regions of the corresponding z-projected and Gaussian
101   filtered images is characterized. Specifically, a characteristic length L_0 of such decay in each R region
102   is extracted, and we interpret this as the fluorescence characteristic domain size. To extract L_0, the
103   mean fluorescence intensity within different concentric subregions within region R around the
104   centroid r_0 is computed; the most central subregion is a circle of radius $d\rho$=1 μm, and the other
105   subregions are 39 concentric i-toroids ($i=1,…39$) filling the R region; the i-th toroid is defined by those
106   pixels whose (x,y) coordinates fulfill the relation $\rho_i^2 < (x-x_0)^2+(y-y_0)^2 \leq \rho_{i+1}^2$, x_0 and y_0 being the
107   coordinates of the centroid r_0 and where $\rho_i=id\rho$. Then, the characteristic length L_0 is extracted by fitting
108   the fluorescence profile to an exponential function of the form [15]

109
$$F(r) = C_0 + C_1 e^{-\left(\frac{r}{L_0}\right)^n} , \qquad (1)$$

110   where C_0 corresponds to the mean autofluorescence levels of the sum slices projection, C_1 is the height
111   of the fluorescent peak, and n is an exponent accounting for the radial decay of the fluorescent
112   domain. C_0, C_1 and n are also determined in the fit.

113   The total fluorescence of the selected domains (referred as signal), M_R, is calculated by

114
$$M_R = \gamma \sum_{i \in R} p_i , \qquad (2)$$

115   where p_i is the pixel intensity levels in the i-th pixel of the sum slices projection, and γ is the resolution
116   in microns squares of the image under study. The γ factor corrects the differences in intensity levels
117   between images that have different resolution. Then, the inferred autofluorescence, B_R, is subtracted
118   from the summed fluorescence in the selected domain, so that the intensity used in the analysis reads

119
$$I_R = M_R - B_R , \qquad (3)$$

120   where $B_R=C_0A_R$, being A_R the area of the R region.

121   We have checked that when fixing the n exponent as the average exponent for all the meristems in a
122   given experiment, we obtained equivalent results for the characteristic length and total fluorescence
123   to the case where the n exponent was a free parameter.

124   The code can be found following this link: https://gitlab.com/slcu/teamHJ/pau/RegionsAnalysis
125   (v0.1)

126

RNA extraction and qPCR:

127

Three biological replicates of three roots each were used in each time-point. Roots were quickly washed in water to remove the sand and terra-green and frozen in liquid nitrogen before being manually ground. Total RNA was extracted using the RNA plus mini kit (Qiagen). First strand cDNA was then synthesized using the Transcriptor First strand cDNA kit (v.6 Roche). Real-time quantitative PCR was performed using double-strand DNA-specific dye SYBR Green (Applied Biosystems) in a LightCycler 480 II (Roche). positive replicates and one negative (using as template a product of the cDNA transcription made without the transcriptase) were performed for each reaction. Expression of *UBQ10*, *NIA1*, *IPT3* and *IPT5* was assessed using the primers described in the following table. Expression data of *NIA1*, *IPT3* and *IPT5* were obtained by normalizing for each replicate the ½ CT of the corresponding gene by the one of *UBQ10*.

138

UBQ10-qPCR-F	AACTTTGGTGGTTTGTGTTTTGG
UBQ10-qPCR-R	TCGACTTGTCATTAGAAAGAAAGAGATAA
NIA1-qPCR-F	GCACGTTTTCGTTTGCGC
NIA1-qPCR-R	GATATGACCAACCGCGTCG
IPT3-pPCR-F	AGACTTCCCTCCAGCGAGAT
IPT3-qPCR-R	GAGAGTCGTGACTTGCCTGT
IPT5-qPCR-F	ACCTAGCCACTCGTTTTCCG
IPT5-qPCR-R	TTCGTAAGTGTCGTGGACGG

139

Cytokinin analysis by mass spectrometry:

Three replicates of three roots, shoots or inflorescences each were used in each condition. Tissues were frozen in liquid nitrogen, ground manually and an aliquot of 100 to 400 mg was taken and weighed. Cytokinins were then extracted and measured by liquid chromatography - mass spectrometry (LC-MS) following the protocol described in [16], with the following modifications: the mass spectrometer was an Applied Biosystems QTrap 6500 system, and the initial mobile phase was 5% acetonitrile in 10 mM ammonium formate (pH3.4).

Grafting:

Arabidopsis micro-grafting was performed on 7-day-old seedlings according to the protocol described in[17]. Grafted seedlings were transferred to soil 7 days after grafting, watered with 1/1/1 fertilizer and put in a constant light room until bolting stage.

In-situ Hybridization

Full length *WUS* cDNA was amplified by PCR using specific primers and ligated into a pGEM-T Easy vector (Promega). Transcription was performed using the DIG RNA labelling kit (Roche). Embedding of the samples, sectioning (8μm sections) and *in situ* hybridization were performed following the protocol described in (http://www.its.caltech.edu/~plantlab/ protocols/insitu.pdf) with the addition of 4% polyvinyl alcohol (PVA) to the nitro blue tetrazolium-bromochloroindolyl phosphate (NBT-BCIP) staining solution. Sections were captured with a 20x lens using an Axioimager microscope (Zeiss) with fully opened diaphragm at 2048 x 2048 picture size. Quantification of the *WUS* expression area was described previously[18]. The threshold was determined by the mean intensity of the unstained tissue of the same section minus four standard deviations. Three consecutive sections that showed the strongest staining signal were analysed per meristem and the expression area was averaged. For

163 *ipt3,5,7* and *cyp735a* the staining signal of two consecutive sections was quantified and averaged,
164 since the *WUS* signal was only detectable in two sections. Image analysis was performed using the
165 ImageJ software.
166
167 **Statistical analysis**

168 Statistical analyses were performed using either Microsoft Excel or R software (https://www.R-
169 project.org). Mean or mode values (for boxplots) were shown with error bars corresponding to the
170 standard deviation for all experiments except for the analysis of the levels of cytokinin species by mass
171 spectrometry where mean was shown with error bars corresponding to the standard error due to the
172 low number of experimental repeats. The number of biological repeats (usually the number of
173 meristems) is displayed in the legend of each figure or within the figure itself. When independent
174 experiments could not be pooled, one independent experiment was shown in the main figures and
175 one in the supplementary material. When applicable, data were fitted using either linear or
176 exponential models depending on the shape of the cloud of points and on the value of the coefficient
177 of determination R^2 and of the p-value of an F-test on the fit. Within the same experiment, the same
178 type of fit was used when comparing data from different genotypes. When Student tests were
179 performed to compare time points and genotypes. The measurements were assumed to have two-
180 tailed distributions and unequal variances and were considered as significantly different when the p-
181 value was lower than 0.05.

182

183 1   Gruel, J. *et al.* An epidermis-driven mechanism positions and scales stem cell niches in
184   plants. *Sci Adv* **2**, e1500989, doi:10.1126/sciadv.1500989 (2016).
185 2   Jonsson, H. *et al.* Modeling the organization of the WUSCHEL expression domain in the shoot
186   apical meristem. *Bioinformatics* **21 Suppl 1**, i232-240, doi:10.1093/bioinformatics/bti1036
187   (2005).
188 3   Besnard, F., Rozier, F. & Vernoux, T. The AHP6 cytokinin signaling inhibitor mediates an
189   auxin-cytokinin crosstalk that regulates the timing of organ initiation at the shoot apical
190   meristem. *Plant Signal Behav* **9** (2014).
191 4   Zurcher, E. *et al.* A robust and sensitive synthetic sensor to monitor the transcriptional
192   output of the cytokinin signaling network in planta. *Plant Physiol* **161**, 1066-1075,
193   doi:10.1104/pp.112.211763 (2013).
194 5   Daum, G., Medzihradszky, A., Suzaki, T. & Lohmann, J. U. A mechanistic framework for
195   noncell autonomous stem cell induction in Arabidopsis. *Proc Natl Acad Sci U S A* **111**, 14619-
196   14624, doi:10.1073/pnas.1406446111 (2014).
197 6   Miyawaki, K. *et al.* Roles of Arabidopsis ATP/ADP isopentenyltransferases and tRNA
198   isopentenyltransferases in cytokinin biosynthesis. *Proc Natl Acad Sci U S A* **103**, 16598-
199   16603, doi:10.1073/pnas.0603522103 (2006).
200 7   Tokunaga, H. *et al.* Arabidopsis lonely guy (LOG) multiple mutants reveal a central role of the
201   LOG-dependent pathway in cytokinin activation. *Plant J* **69**, 355-365, doi:10.1111/j.1365-
202   313X.2011.04795.x (2012).
203 8   Melnyk, C. W., Schuster, C., Leyser, O. & Meyerowitz, E. M. A Developmental Framework for
204   Graft Formation and Vascular Reconnection in Arabidopsis thaliana. *Curr Biol* **25**, 1306-1318,
205   doi:10.1016/j.cub.2015.03.032 (2015).
206 9   Wilson, A. K., Pickett, F. B., Turner, J. C. & Estelle, M. A dominant mutation in Arabidopsis
207   confers resistance to auxin, ethylene and abscisic acid. *Mol Gen Genet* **222**, 377-383 (1990).
208 10   Muller, D. *et al.* Cytokinin is required for escape but not release from auxin mediated apical
209   dominance. *Plant J* **82**, 874-886, doi:10.1111/tpj.12862 (2015).

210   11   Siligato, R. *et al.* MultiSite Gateway-Compatible Cell Type-Specific Gene-Inducible System for
211   Plants. *Plant Physiol* **170**, 627-641, doi:10.1104/pp.15.01246 (2016).
212   12   Smyth, D. R., Bowman, J. L. & Meyerowitz, E. M. Early flower development in Arabidopsis.
213   *Plant Cell* **2**, 755-767, doi:10.1105/tpc.2.8.755 (1990).
214   13   Fernandez, R. *et al.* Imaging plant growth in 4D: robust tissue reconstruction and lineaging at
215   cell resolution. *Nat Methods* **7**, 547-553, doi:10.1038/nmeth.1472 (2010).
216   14   Landrein, B. *et al.* Meristem size contributes to the robustness of phyllotaxis in Arabidopsis. *J
217   Exp Bot* **66**, 1317-1324, doi:10.1093/jxb/eru482 (2015).
218   15   Bergmann, S. *et al.* Pre-steady-state decoding of the Bicoid morphogen gradient. *PLoS Biol* **5**,
219   e46, doi:10.1371/journal.pbio.0050046 (2007).
220   16   Young, N. F. *et al.* Conditional Auxin Response and Differential Cytokinin Profiles in Shoot
221   Branching Mutants. *Plant Physiol* **165**, 1723-1736, doi:10.1104/pp.114.239996 (2014).
222   17   Melnyk, C. W. Grafting with Arabidopsis thaliana. *Methods Mol Biol* **1497**, 9-18,
223   doi:10.1007/978-1-4939-6469-7_2 (2017).
224   18   Geier, F. *et al.* A quantitative and dynamic model for plant stem cell regulation. *PLoS One* **3**,
225   e3553, doi:10.1371/journal.pone.0003553 (2008).

226